Title

Regional wall stress differences on tricuspid aortic valve-associated ascending aortic aneurysms

Journal

Interdisciplinary CardioVascular and Thoracic Surgery, 34(6)

ISSN

1569-9293

Authors

Gomez, Axel

Wang, Zhongjie

Xuan, Yue

et al.

Publication Date

2022-06-01

DOI

10.1093/icvts/ivab269

Peer reviewed

Interactive CardioVascular and Thoracic Surgery 34 (2022) 1115–1123
doi:10.1093/icvts/ivab269 Advance Access publication 30 October 2021

ORIGINAL ARTICLE

Cite this article as: Gomez A, Wang Z, Xuan Y, Hope MD, Saloner DA, Guccione JM *et al*. Regional wall stress differences on tricuspid aortic valve-associated ascending aortic aneurysms. Interact CardioVasc Thorac Surg 2022;34:1115–23.

Regional wall stress differences on tricuspid aortic valve-associated ascending aortic aneurysms

Axel Gomez[a], Zhongjie Wang [a], Yue Xuan[a], Michael D. Hope[b], David A. Saloner[b], Julius M. Guccione[a], Liang Ge[a] and Elaine E. Tseng [a,*]

[a] Division of Adult Cardiothoracic Surgery, Department of Surgery, University of California San Francisco and San Francisco VA Medical Center, San Francisco, CA, USA
[b] Department of Radiology, University of California San Francisco and San Francisco VA Medical Center, San Francisco, CA, USA

* Corresponding author. Division of Adult Cardiothoracic Surgery, Department of Surgery, University of California San Francisco and San Francisco VA Medical Center, 500 Parnassus Ave. Suite 405W, San Francisco, CA 94143, USA. Tel: +1-415-2214810, x23452; fax: +1-415-7502181; e-mail: elaine.tseng@ucsf.edu (E.E. Tseng).

Received 15 February 2021; received in revised form 15 July 2021; accepted 27 August 2021

Key question

What anatomic regions experience the highest wall stresses in aTAAs associated with a tricuspid aortic valve?

Key finding(s)

Circumferential and longitudinal wall stresses are greatest at the aortic root for patients with TAV-aTAA.

Take-home message

Finite element analysis may be clinically used to assess patient-specific dissection risk based on regional wall stress-to-strength ratios.

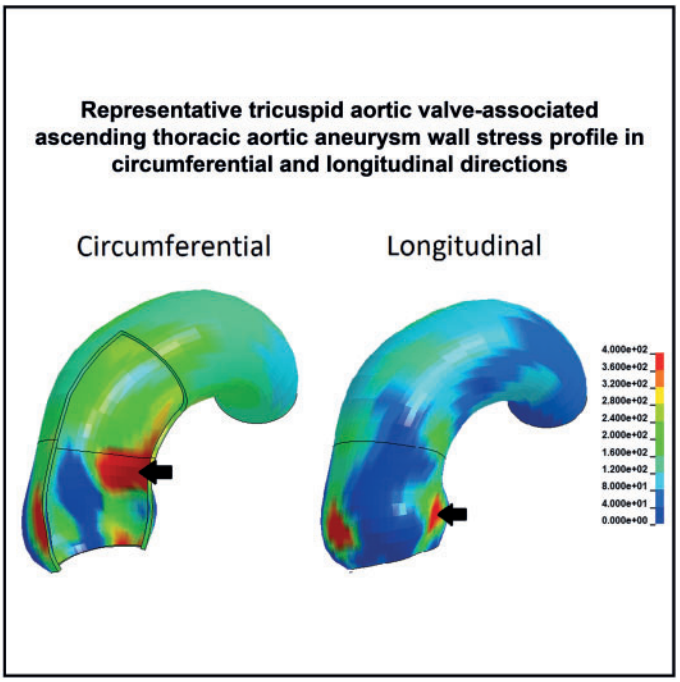

VASCULAR

Abstract

OBJECTIVES: Ascending thoracic aortic aneurysms (aTAAs) carry a risk of acute type A dissection. Elective repair guidelines are based on diameter, but complications often occur below diameter threshold. Biomechanically, dissection can occur when wall stress exceeds wall strength. Aneurysm wall stresses may better capture dissection risk. Our aim was to investigate patient-specific aTAA wall stresses associated with a tricuspid aortic valve (TAV) by anatomic region.

Presented at the American College of Surgeons Clinical Congress 2020, 3–7 October 2020, Virtual.

METHODS: Patients with aneurysm diameter ≥4.0 cm underwent computed tomography angiography. Aneurysm geometries were reconstructed and loaded to systemic pressure while taking prestress into account. Finite element analyses were conducted to obtain wall stress distributions. The 99th percentile longitudinal and circumferential stresses were determined at systole. Wall stresses between regions were compared using one-way analysis of variance with *post hoc* Tukey HSD for pairwise comparisons.

RESULTS: Peak longitudinal wall stresses on aneurysms ($n = 204$) were 326 [standard deviation (SD): 61.7], 246 (SD: 63.4) and 195 (SD: 38.7) kPa in sinuses of Valsalva, sinotubular junction (STJ) and ascending aorta (AscAo), respectively, with significant differences between AscAo and both sinuses ($P < 0.001$) and STJ ($P < 0.001$). Peak circumferential wall stresses were 416 (SD: 85.1), 501 (SD: 119) and 340 (SD: 57.6) kPa for sinuses, STJ and AscAo, respectively, with significant differences between AscAo and both sinuses ($P < 0.001$) and STJ ($P < 0.001$).

CONCLUSIONS: Circumferential and longitudinal wall stresses were greater in the aortic root than AscAo on aneurysm patients with a TAV. Aneurysm wall stress magnitudes and distribution relative to respective regional wall strength could improve understanding of aortic regions at greater risk of dissection in a particular patient.

Keywords: Aortic aneurysm • Wall stress • Finite element analysis

ABBREVIATIONS

AscAo	Ascending aorta
aTAA	Ascending thoracic aortic aneurysm
BAV	Bicuspid aortic valve
CTA	Computer tomography angiography
FE	Finite element
SD	Standard deviation
STJ	Sinotubular junction
TAV	Tricuspid aortic valve

INTRODUCTION

Most ascending thoracic aortic aneurysms (aTAAs) are sporadic and associated with a tricuspid aortic valve (TAV) [1]. Despite more frequent aTAA diagnoses and guidelines for elective repair, ∼2–3% of patients experience dissection/rupture events per year [2], which carry 11–18% perioperative mortality in patients that reach the hospital alive [3, 4]. aTAA repair guidelines use diameter cut-offs balancing risk of dissection with that of surgery. The American College of Cardiology/American Heart Association recommend elective surgical replacement for diameter ≥5.5 cm with earlier intervention for rapid growth rate, connective tissue disorder, family history of dissection and concomitant surgery [5]. Our laboratory and others have reported that ∼60–90% of type A dissection events occur in aTAAs with diameter <5.5 cm and otherwise not meeting elective surgical repair indications [6–8]. There is an unmet need for patient-specific aTAA repair criteria that accurately captures dissection risk in aneurysms of all sizes.

Laplace's Law describes wall stress of cylindrical structures as proportional to diameter. Diameter serves as a surrogate for aTAA wall stress, where dissection can occur from aortic wall failure when wall stresses exceed wall strength [9]. However, Laplace's law does not accurately estimate wall stresses in complex aTAA geometries. Accurate patient-specific wall stress profiles could significantly enhance understanding and prediction of aTAA complications. Unfortunately, wall stresses cannot be directly measured *in vivo*. Finite element (FE) analysis is a validated computational technique to determine patient-specific wall stress profiles. We previously studied bicuspid aortic valve (BAV)-aTAA wall stresses by anatomic region to assess vulnerability when combined with complementary wall strength data [1]. The aim of this study was to determine wall stress magnitudes of TAV-aTAAs in relationship to anatomic regions.

MATERIAL AND METHODS

Study participants

aTAA patients with maximum diameter ≥4.0 cm were included from the San Francisco Veterans Affairs Medical Center (SFVAMC). Patients with BAV, connective tissue disorder, prior cardiac surgical intervention or isolated aortic root/arch dilatation were excluded. Patients with at least 1 computer tomography angiography (CTA) scan and aneurysm diagnosis were included in the study. Patients with aneurysm surgery had a CTA scan prior to surgery used for analysis. This study was approved by the Committee on Human Research at University of California San Francisco Medical Center and Institutional Review Board at SFVAMC. Informed consent was not required from the large cohort population as the protocols approved allowed retrospective review of imaging and clinical data.

Geometry reconstruction and finite element modelling

Patient-specific 3-dimensional TAV-aTAA geometries were reconstructed from CTA images using MeVisLab software (MeVis Medical Solutions AG, Bremen, Germany). All modelled CTA images preceded any aortic intervention. Models included left ventricular outflow tract, aortic annulus, sinuses of Valsalva, sinotubular junction (STJ), ascending aorta (AscAo), aortic arch and portion of the descending thoracic aorta. Aortic arch branches were not included. Models were then imported into TrueGrid software (version 3.1.3; XYZ Scientific, Inc., Livermore, CA, USA) to create a geometric mesh with 11 202 hexahedral elements and uniform 1.80 mm thickness. Geometric meshes had 3 layers reflecting aortic intima, media and adventitia. LS-DYNA R10 (LSTC Inc., Livermore, CA, USA) was used for FE pressure loading simulations and analysis.

Initial aTAA models had geometries at systemic pressure. A modified update-Lagrangian method was applied to account for this prestress and obtain zero-pressure geometries suitable for FE simulations [10]. aTAA wall was modelled as incompressible hyperelastic material with a user-defined collagen-embedded material model [11]. Average population TAV-specific aTAA material properties were derived from previous stretch testing [12]. To allow for aortic movement during the cardiac cycle while considering restraint from the ligamentum arteriosum, we fixed translational motion at the left ventricular outflow tract (20 mm proximal to the aortic annulus) and distally at the descending thoracic aorta. No constraints to rotational motion were placed.

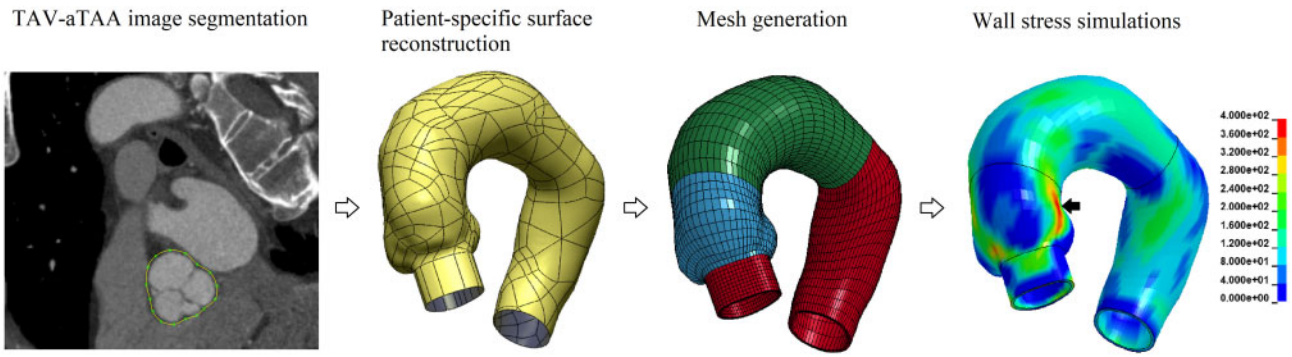

Figure 1: Schematic representation of finite element modelling process: image segmentation of a sample TAV-aTAA, patient-specific ascending thoracic aortic aneurysm surface reconstruction (yellow), geometric mesh creation with anatomic regions defined in colour and wall stress distribution with peak systolic stress (black arrow). TAV-aTAA: tricuspid aortic valve-associated ascending thoracic aortic aneurysm.

FE simulations were performed by applying human physiological arterial pressure conditions to aTAA inner lumen. Simulations started with an initial lumen pressurization to 80 mmHg. The cardiac cycle was subsequently simulated by a gradual increase in pressure from 80 to 120 mmHg over 300 ms followed by a decrease back to 80 mmHg over an additional 500 ms. Reproducibility was tested with 2 independent investigators reconstructing TAV-aTAA models for a 25% patient subset and running FE simulations. Figure 1 provides a process schematic of TAV-aTAA geometry reconstruction and FE simulations.

Data and statistical analysis

Statistical analysis was performed utilizing 99th percentile wall stresses to avoid inhomogeneities in the models [13]. Peak wall stresses will heretofore refer to 99th percentile wall stresses. Peak circumferential and longitudinal wall stresses were calculated at sinuses, STJ and AscAo. Effect of region on peak wall stress was studied with one-way repeated measures analysis of variance with Greenhouse–Geisser correction for sphericity departure. When analysis of variance found statistically significant effect of region on peak stress, *post hoc* Tukey HSD test was implemented for pairwise comparison of regions. For STJ and AscAo, we also studied the effect of curvature, either greater or lesser, on peak stress. Comparisons of peak stress between curvatures at a single region were performed with a paired sample *t*-test. TAV-aTAA models were classified by STJ effacement, aortic valve disease and diameter. For each classification system, peak wall stresses were compared at different regions using unpaired sample *t*-tests. Continuous variables are reported as mean and standard deviation (SD). Categorical variables are reported with count and percentages. A *P*-value <0.05 was considered statistically significant. Statistical analyses were performed using R software by a single investigator (http://www.r-project.org). The raw wall stress data will be shared on reasonable request to the corresponding author.

RESULTS

Patient characteristics

A total of 204 TAV-aTAA patients had a mean age of 69 (SD: 7.7) years. The mean aTAA diameter was 4.62 (SD: 0.55) cm. Majority of patients were male (97.1%). The most common co-morbidities were hypertension (77.9%), hyperlipidaemia (71.1%) and chronic obstructive pulmonary disease (25.5%). Patient characteristics are presented in Table 1.

Wall stress by anatomic region

Peak wall stress differed between regions for both circumferential ($F = 160$, $P < 0.001$) and longitudinal ($F = 287$, $P < 0.001$) directions. Peak circumferential wall stresses were 416 (SD: 85.1) kPa at sinuses, 501 (SD: 119) kPa at STJ and 340 (SD: 57.6) kPa at AscAo. Circumferential stresses were lower at the AscAo than sinuses ($P < 0.001$) and STJ ($P < 0.001$). STJ had greater circumferential peak stresses than the sinuses ($P < 0.001$). Locations of peak circumferential wall stresses were the sinuses in 35 (17.2%), STJ in 164 (80.4%) and AscAo in 5 (2.5%) of TAV-aTAAs. Circumferential peak stresses by region are illustrated in Fig. 2A. Peak longitudinal wall stresses were 326 (SD: 61.7) kPa at sinuses, 246 (SD: 63.4) kPa at STJ and 195 (SD: 38.7) kPa at AscAo. Longitudinal stresses were also lower at the AscAo than sinuses ($P < 0.001$) and STJ ($P < 0.001$). Sinuses had greater longitudinal stresses than STJ ($P < 0.001$). Locations of peak longitudinal wall stresses were the sinuses in 192 (94.1%) and STJ in 12 (5.9%) of TAV-aTAAs. Longitudinal peak stresses are shown in Fig. 2B. Overall, peak circumferential wall stresses for TAV-aTAAs were greater in the circumferential than longitudinal direction [509 (SD: 111) vs 318 (SD: 57.7) kPa, $P < 0.001$]. The same relationship was true for the sinuses ($P < 0.001$), STJ ($P < 0.001$) and AscAo ($P < 0.001$). A representative TAV-aTAA wall stress profile of a specific patient is shown illustrating the overall relationships found in this study (Fig. 3). Wall stress values for the overall patient cohort and also by groups of aTAA size <5.5 vs ≥5.5 cm are shown in Table 2.

Wall stresses along greater versus lesser curvature

For the AscAo, peak circumferential and longitudinal wall stresses were larger in the lesser than greater curvature 342 (SD: 55.5) vs 286 (SD: 45.0) kPa, $P < 0.001$, and 190 (SD: 42.1) vs 174 (SD: 28.8) kPa, $P < 0.001$, respectively. Similarly, for STJ, peak circumferential and longitudinal wall stresses were higher in the lesser than greater curvature 502 (SD: 121) vs 366 (SD: 74.4) kPa, $P < 0.001$,

Table 1: Population characteristics

Characteristics	TAV-aTAA ($n = 204$)
Maximum diameter (cm), mean (SD)	4.62 (0.55)
Sinuses of Valsalva diameter ($n = 149$), mean (SD)	4.32 (0.56)
Sinotubular junction diameter ($n = 149$), mean (SD)	3.67 (0.56)
Mid-ascending aorta diameter ($n = 149$), mean (SD)	4.34 (0.51)
Age (years), mean (SD)	69 (7.7)
Male gender, n (%)	198 (97.1)
Smoking (pack-years), mean (SD)	25 (26)
Hypertension, *n* (%)	159 (77.9)
Diabetes, *n* (%)	37 (18.1)
Hyperlipidaemia, *n* (%)	145 (71.1)
CAD, *n* (%)	39 (19.1)
PVD, *n* (%)	19 (9.3)
COPD, *n* (%)	52 (25.5)
CVA, *n* (%)	14 (6.9)
CKD, *n* (%)	21 (10.3)
Carotid stenosis, *n* (%)	3 (1.5)
Arrhythmia, *n* (%)	62 (30.4)
MI, *n* (%)	13 (6.4)
LVEF (%), mean (SD)	61 (8.2)
NYHA class CHF, *n* (%)	12 (5.9)
Class I	6 (2.9)
Class II	3 (1.5)
Class III	3 (1.5)
Class IV	0 (0)
Haemodialysis, *n* (%)	1 (0.5)
Prior PCI, *n* (%)	15 (7.4)
Aortic stenosis, *n* (%)	
None	151 (74.0)
Mild	6 (2.9)
Moderate	2 (1.0)
Severe	2 (1.0)
Data not available	43 (21.1)
Aortic insufficiency, *n* (%)	
None	109 (53.4)
Mild	32 (15.7)
Moderate	12 (5.9)
Severe	8 (3.9)
Data not available	43 (21.1)

CAD: coronary artery disease; CHF: congestive heart failure; CKD: chronic kidney disease; COPD: chronic obstructive pulmonary disease; CVA: cerebrovascular accident; LVEF: left ventricular ejection fraction; MI: myocardial infarction; NYHA: New York Heart Association; PCI: percutaneous coronary intervention; PVD: peripheral vascular disease; SD: standard deviation; TAV-aTAA: tricuspid aortic valve-associated ascending thoracic aortic aneurysm.

and 231 (SD: 65.4) vs 220 (SD: 58.1) kPa, $P = 0.002$, respectively. Representative curvatures stress profiles are shown (Fig. 3).

Wall stresses based upon STJ effacement

For 149 (73.0%) TAV-aTAAs with available size measurements of sinuses, STJ and AscAo, STJ effacement was present in 81 (54.4%) of patients. aTAAs with STJ effacement had an overall smaller diameter than those without effacement [4.5 (SD: 0.39) vs 4.7 (SD: 0.60) kPa, $P = 0.008$]. Longitudinal peak stresses between the effaced and non-effaced STJ phenotypes were 318 (SD: 52.7) vs 336 (SD: 70.2) kPa ($P = 0.10$) at the sinuses, 235 (SD: 53.0) vs 251 (SD: 70.7) kPa ($P = 0.12$) at STJ and 191 (SD: 33.9) vs 196 (SD: 42.1) kPa ($P = 0.48$) at AscAo, respectively. Circumferential peak stresses between the effaced and non-effaced STJ phenotypes were 401 (SD: 68.2) vs 424 (SD: 87.7) kPa ($P = 0.08$) at the sinuses, 487 (SD: 102) vs 515 (SD: 138) kPa ($P = 0.17$) at STJ and 326 (SD: 45.9) vs 353 (SD: 70.3) kPa ($P = 0.008$) at AscAo, respectively. Representative wall stress profiles in specific patients of similar aneurysm size but with and without STJ effacement are shown (Fig. 4).

Wall stresses based upon aortic valve disease

For 161 (78.9%) TAV-aTAAs with echocardiographic data, 10 (6.2%) patients had some degree of aortic stenosis and 52 (32.3%) patients had aortic insufficiency. Circumferential and longitudinal wall stresses were similar among aTAAs with and without aortic stenosis (Table 3). Patients with aortic stenosis had an overall similar diameter than those without [4.7 (SD: 0.75) vs 4.7 (SD: 0.57) kPa, $P = 0.76$]. Circumferential and longitudinal wall stresses were greater in aTAAs with aortic insufficiency than those without (Table 3). Patients with aortic insufficiency had an overall greater diameter than those without [5.0 (SD: 0.66) vs 4.5 (SD: 0.47) cm, $P < 0.001$]. Representative wall stress profiles in specific patients with and without aortic stenosis or aortic insufficiency are shown (Fig. 5).

Reproducibility of results was evaluated by comparing FE simulation results of TAV-aTAA models constructed independently by 2 investigators for $n = 51$ (25%) patients. The inter-investigator variability had a percentage difference of 4% (SD: 4%) for circumferential peak wall stresses ($P = 0.51$) and 5% (SD: 3%) for longitudinal peak wall stresses ($P = 0.14$).

DISCUSSION

Acute type A dissection is a surgical emergency with ∼25% prehospital and 11–18% surgical mortality rates [3, 4]. From a biomechanical standpoint, dissection represents aortic wall failure when wall stresses exceed wall strength. In our study, we found higher longitudinal wall stresses in the root with location of peak stresses occurring at the sinuses the majority of the time followed by STJ. Studying patient-specific wall stress profiles in relation to regional strength variation can help identify TAV-aTAA patients at risk of dissection and aortic regions vulnerable to an initial intimal tear.

Wall stress profiles

In this study, we found that the magnitudes of TAV-aTAA peak wall stresses were greater in the aortic root than AscAo. Both STJ and sinuses experienced larger circumferential and longitudinal wall stresses than AscAo. A limited number of FE analysis studies have evaluated TAV-aTAA wall stress distributions. Consistent with our findings, Jackson *et al.* reported that in 20 TAV-aTAAs, locations of 99th percentile Von Mises wall stresses were just above the right or left coronary sinuses in 80% versus AscAo in remaining 20% of patients [14]. Their study was limited by small sample size, lack of *in vivo* prestressed geometry correction and peak stress general locations without defining magnitudes and differences between aortic regions. Similarly, Pasta *et al.* [15] found that a local wall principal stress maxima was present just above the STJ in TAV-aTAAs with 2 additional foci of increased stresses in AscAo without comparison to STJ magnitudes. Average principal wall stresses in the anterolateral aorta were 230 kPa in AscAo, 300 kPa in STJ and 180 kPa in aortic annulus.

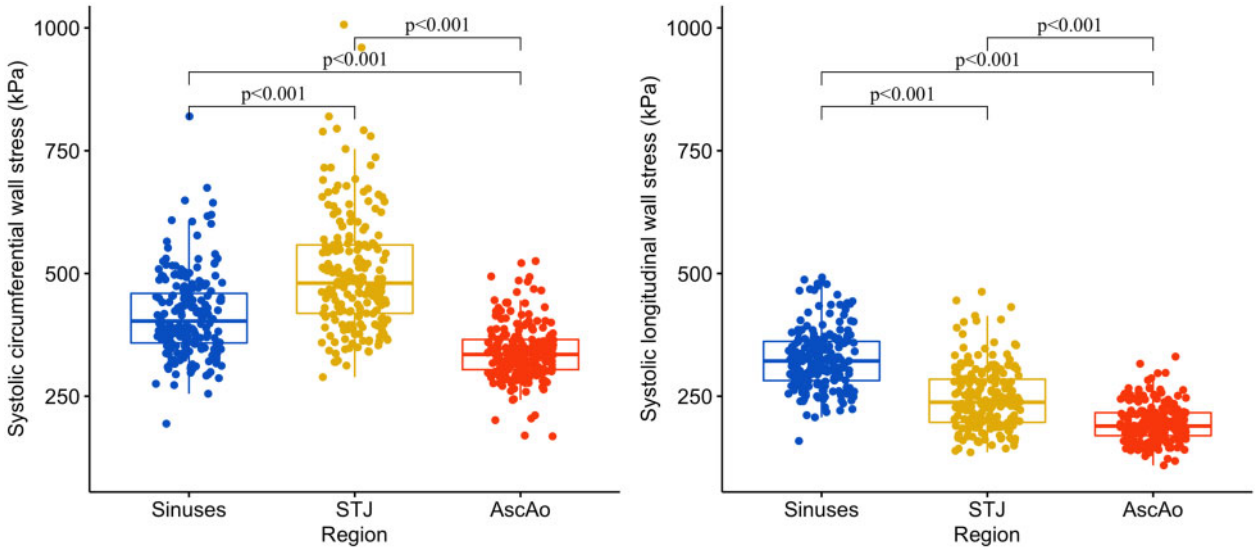

Figure 2: Box plots representing relationship of peak circumferential (**A**) and longitudinal (**B**) wall stresses and ascending thoracic aortic aneurysm region at systolic pressure. Median (horizontal line), 25th and 75th percentiles (box), range (whiskers) and observations (dots). AscAo: ascending aorta; STJ: sinotubular junction.

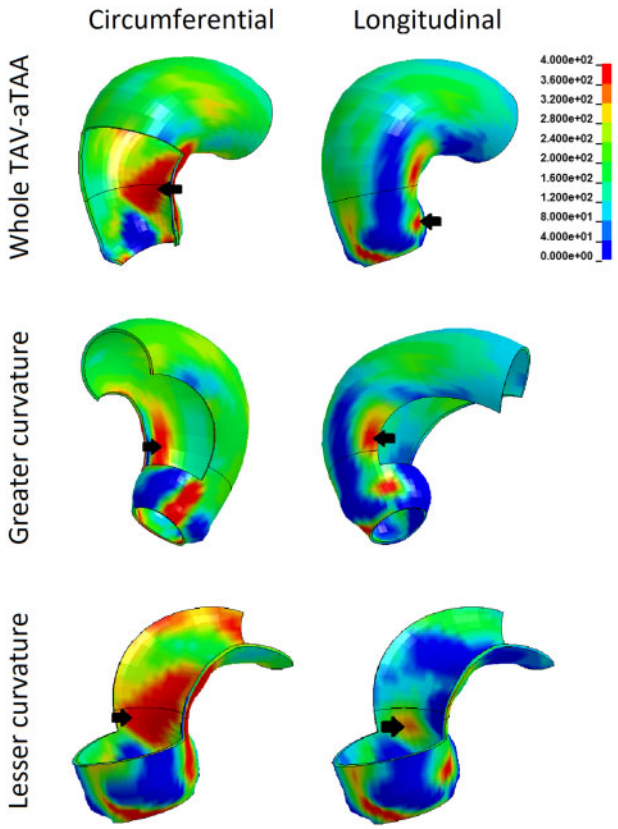

Figure 3: Representative TAV-aTAA wall stress profiles in both circumferential and longitudinal directions for whole aneurysm geometry, greater curvature and lesser curvature. TAV-aTAA: tricuspid aortic valve-associated ascending thoracic aortic aneurysm.

Consistent with our results, STJ experienced overall higher first principal wall stresses than AscAo. However, they potentially masked sub-regions of higher stresses when averaged with smaller stresses in the same region. Our findings are also consistent with our earlier results of smaller sample size. In our previous study, we found that for a cohort of ~100 aTAAs, peak wall stresses were largest at the aortic root for both longitudinal and circumferential directions [11]. In particular, the STJ experienced the largest circumferential stresses. These findings remained true when examining aneurysms of either size <5.0 or ≥5 cm. However, both BAV- and TAV-aTAAs were included, while our current study focuses exclusively on TAV-aTAAs, with double the sample size. Notably, in this study, we re-examined the effect of size on wall stress profiles and noted that TAV-aTAAs <5.5 and ≥5.5 cm share a regional stress distribution pattern only differing by a greater magnitude in the larger aneurysms. Patterns of high wall stresses in STJ and root are not unique to TAV-aTAAs and have also been reported in BAV-aTAAs and non-aneurysmal aorta [1, 16]. Clinically, the location of the initial intimal tear is often at or near the STJ [8]. Current evidence seems to suggest that the aortic root especially at the STJ, regardless of aortic valve phenotype, experiences the largest wall stress in aTAAs and depending on corresponding strength of aortic root may provide insight into the proclivity for biomechanical failure.

In our study, we found that TAV-aTAA lesser curvature experienced higher wall stresses than the greater curvature in both STJ and AscAo. Difference in peak wall stresses between greater and lesser curvature was higher in the circumferential than longitudinal directions. Longitudinal peak wall stress differences between the 2 curvatures were minor, <10% of their absolute values for both STJ and AscAo; thus, this statistically significant difference is unlikely to be clinically significant. In contrast, circumferential wall stress differences between the 2 curvatures had a more substantial ~20% difference from their absolute magnitudes. Figure 3 shows a representative specific patient with their wall stress profile that presents these relationships. Our results are consistent with previous small studies [17]. Avril *et al.* found that the maximal principal wall stresses were located in the inner curvature for all 5 patients of their study [17]. That study was limited by their small sample size and because their aneurysm geometries were limited to AscAo and STJ, excluding sinuses and left ventricular outflow tract, wall stress values may have been affected by their boundary conditions. Our group also previously studied and reported differences in wall stresses between greater and lesser

Table 2: TAV-aTAA peak wall stresses upon diameter

	All aTAAs (n = 204)	aTAAs <5.5 cm (n = 183)	aTAAs ≥5.5 cm (n = 21)	P-value between aTAAs <5.5 and ≥5.5 cm
Circumferential wall stresses				
Sinuses of Valsalva (kPa), mean (SD)	416 (85.1)	404 (73.7)	518 (108)	<0.001
Sinotubular junction (kPa), mean (SD)	501 (119)	486 (108)	627 (135)	<0.001
AscAo (kPa), mean (SD)	340 (57.6)	330 (48.6)	431 (50.6)	<0.001
F-value	160	173	18.7	
P-values between regions				
Sinuses versus STJ	<0.001	<0.001	0.003	
Sinuses versus AscAo	<0.001	<0.001	0.02	
STJ versus AscAo	<0.001	<0.001	<0.001	
Longitudinal wall stresses				
Sinuses of Valsalva (kPa), mean (SD)	326 (61.7)	317 (54.1)	402 (72.3)	<0.001
Sinotubular junction (kPa), mean (SD)	246 (63.4)	236 (55.5)	331 (64.9)	<0.001
AscAo (kPa), mean (SD)	195 (38.7)	190 (35.7)	240 (33.9)	<0.001
F-value	287	315	39.1	
P-values between regions				
Sinuses versus STJ	<0.001	<0.001	<0.001	
Sinuses versus AscAo	<0.001	<0.001	<0.001	
STJ versus AscAo	<0.001	<0.001	<0.001	

[a]TAA: ascending thoracic aortic aneurysm; AscAo: ascending aorta; SD: standard deviation; STJ: sinotubular junction; TAV-aTAA: tricuspid aortic valve-associated ascending thoracic aortic aneurysm.

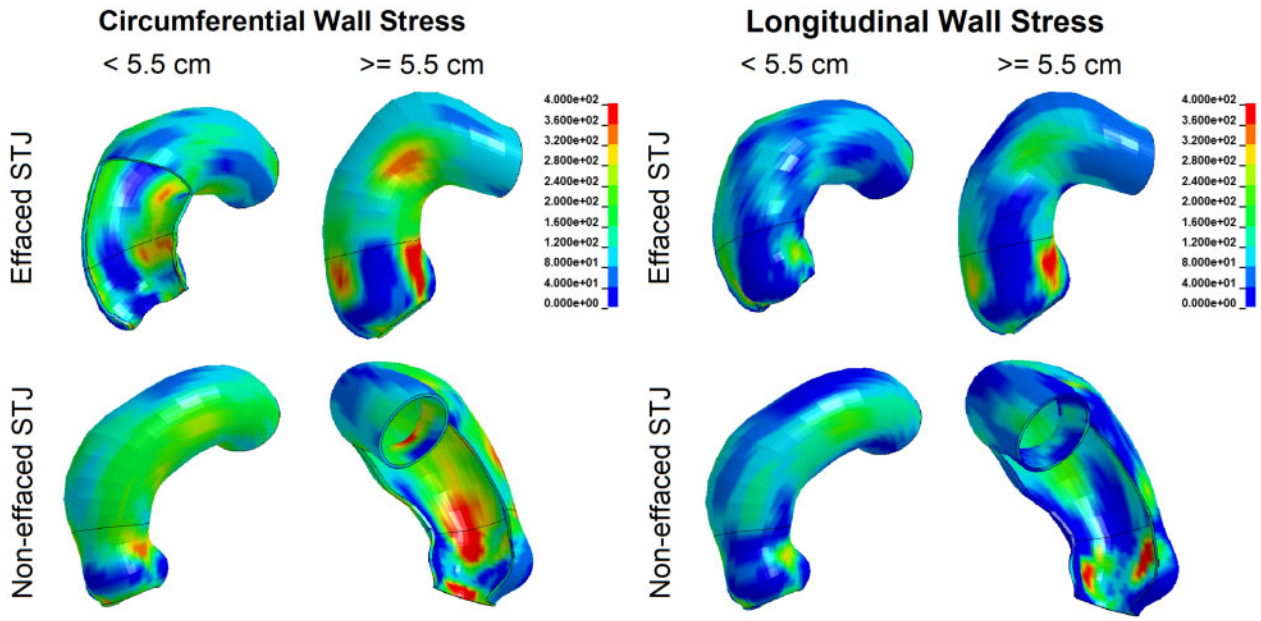

Figure 4: Representative circumferential (**A**) and longitudinal (**B**) wall stress profiles of small and large ascending thoracic aortic aneurysms with and without STJ effacement. STJ: sinotubular junction.

curvatures in TAV-aTAAs. Xuan *et al.* [18] studied 17 TAV-aTAAs and found that circumferential but not longitudinal wall stresses were larger in the lesser curvature for the AscAo. Our current study adds stronger evidence of higher wall stresses in the lesser than greater curvature at a population level. Lastly, these results are not inconsistent with the observation of larger expansion along the greater versus lesser curvature during systole. Higher circumferential stress at the lesser curvature was also observed by Gleason *et al.* [19]. Due to the non-linear material property of soft tissue, the relative tissue stiffness increases as stress increases. Regions of higher stress could lead to smaller observable deformation.

We were also interested in exploring the effect of TAV-aTAA morphology on wall stress. We defined STJ effacement by the presence of sinuses/STJ or AscAo/STJ diameter ratios smaller than otherwise expected from normal size variation [20]. Overall, we found that STJ effacement did not impact wall stress magnitudes outside of what would be accounted by differences in diameter. This is in agreement with prior observations in the BAV-aTAAs counterparts [1]. However, we are not aware of any other studies that have looked at this relationship in TAV-aTAAs. In addition, we inspected the effect of a pathological aortic valve on wall stress. We found that aortic stenosis did not appear to affect magnitudes of wall stress, but it was noted that patients with

Table 3: TAV-aTAA peak wall stresses upon aortic valve disease

	Aortic stenosis			Aortic insufficiency		
	Present (n = 10), mean (SD)	Absent (n = 151), mean (SD)	P-value	Present (n = 52), mean (SD)	Absent (n = 109), mean (SD)	P-value
Circumferential wall stresses						
Sinuses of Valsalva (kPa)	398 (102)	421 (88.1)	0.51	438 (87.1)	411 (88.7)	0.07
Sinotubular junction (kPa)	466 (86.7)	506 (127)	0.20	558 (137)	478 (110)	<0.001
Ascending aorta (kPa)	340 (52.5)	344 (61.0)	0.80	378 (66.9)	328 (49.7)	<0.001
Longitudinal wall stresses						
Sinuses of Valsalva (kPa)	348 (84.2)	327 (63.5)	0.45	351 (63.1)	317 (63.0)	0.002
Sinotubular junction (kPa)	242 (57.7)	248 (66.8)	0.77	275 (71.0)	235 (59.6)	<0.001
Ascending aorta (kPa)	202 (41.8)	196 (40.3)	0.63	213 (36.3)	188 (39.7)	<0.001

SD: standard deviation; TAV-aTAA: tricuspid aortic valve-associated ascending thoracic aortic aneurysm.

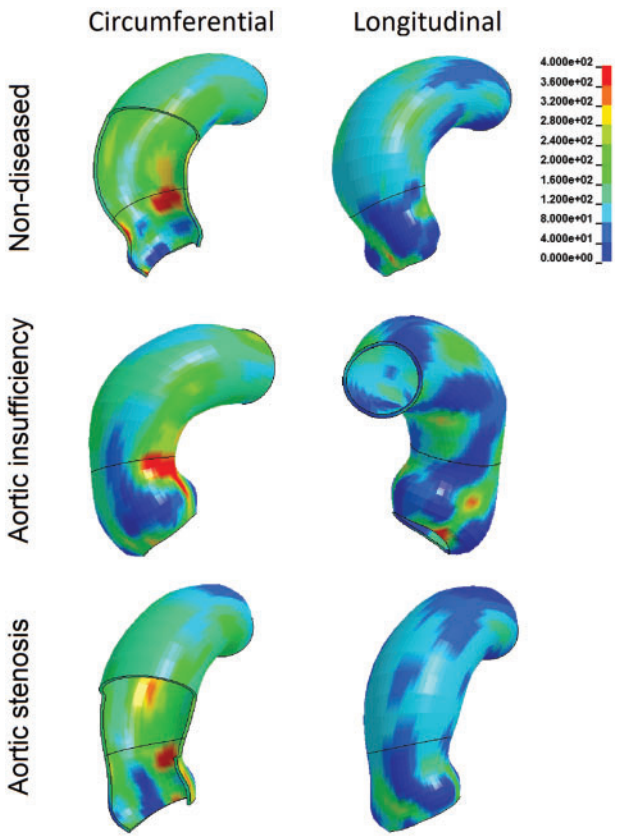

Figure 5: Representative ascending thoracic aortic aneurysm wall stress profiles in both circumferential and longitudinal directions for aneurysms with either aortic stenosis, aortic insufficiency or disease-free aortic valve.

aortic insufficiency experienced larger wall stress than those without disease. An overall larger diameter in the aortic insufficiency group likely contributed to the increased stress, but this observation has been reported in prior studies where a larger axial root displacement was also identified as a key contributor [21].

Our study fills a substantial gap in knowledge regarding wall stress profiles in TAV-aTAAs. Measuring patient-specific wall stress distributions and peak magnitudes through computational modelling could be helpful at identifying patients and aneurysm regions at increased risk of dissection when considering their wall stress in relation to their respective strength. Our findings of high circumferential and longitudinal peak wall stresses in the aortic root and lesser curvature suggest regions that may be at risk of intimal tears if the magnitudes of wall stresses are substantially greater than that in the normal population or exceed the wall strength in those regions. We demonstrated the reproducibility of our methodology and results by having 2 independent investigators perform FE simulations in 25% of the subjects with consistent findings between them.

Intimal tear location

In acute dissection, the initial entry site can occur in various locations in the thoracic aorta with distribution varying between studies [8, 22, 23]. In our published experience, we observed that aortic intimal tears by CT were located in the STJ in 29%, AscAo in 29%, sinuses in 18% and remainder in the arch [8]. Not all tears on CT were documented and confirmed in the intraoperative reports, but for those that were, 1 tear in the AscAo was not detected on CT but found at operation. Most studies did not clearly separate out the regions, i.e. root, STJ, AscAo, but in 2 studies that specified the root separately from the AscAo, the intimal tear rates at the root were 24% [23, 24]. Januzzi *et al.* [23] reported that for ∼1000 patients, tears in the root were more frequent in younger patients, 29% for patients <40 years old versus 23% when patients were >40 years old. High wall stresses at the aortic root may play a role in this finding. Younger patients also had more frequent dissection at the STJ when that region was specifically evaluated separately from AscAo, with 21% tears when patients were <40 and only 7% tears when >40 years old. Unfortunately, the study did not report rates for TAV patients independently. In contrast in another study of ∼400 patients that presented with acute type A dissection, location of initial intimal tear was much more frequent in the AscAo versus aortic root (88% vs 12%, respectively) [22], which remained similar in proportion when exclusively examining TAV patients. One study has found that regions of high wall stress overlapped with the intimal tear locations of their dissection patients [25]. Our results found much higher longitudinal stresses in sinuses than in STJ and

AscAo. These results are consistent with the observation of aortic root as a common initial dissection site. Nevertheless, the AscAo has been reported as the most common aortic tear location in many studies. The location of initial intimal tear not only depends on wall stress but also on wall strength. Regional patterns of wall strength in relation to wall stress could help explain this apparent discrepancy among studies regarding the distribution of intimal tear. Regional wall strength data coupled with wall stresses may be used clinically to determine not only patient-specific risk of dissection but also specific regions most vulnerable to initial intimal tear.

Another proposed hypothesis is that the embryological myocardium-smooth muscle junctions are potential sites for dissection [26]. The first junction is located at the level of the semilunar valves, corresponding to the sinuses. The second junction is located in the proximal AscAo ∼2 cm above the root. These locations do align nicely to our results as we have found that peak wall stresses are the highest in the aortic root. In addition, we have observed that wall stresses tend to be higher near than STJ, which can be appreciated in Fig. 3 which displays representative wall stress profiles.

Aneurysm wall strength properties

Overall, limited data exist presently for regional aortic failure data on a population level. Gasser *et al.* [27] reported that the first Piola-Kirchoff failure stress for TAV-aTAA was 0.49 MPa. On the other hand, Gleason's group found TAV-aTAA wall tensile strength from direct force application to aneurysmal tissue [9]. TAV-aTAA were stronger in the circumferential (1656 kPa) than longitudinal direction (698 kPa). This larger circumferential than longitudinal tensile strength has been corroborated by others, which explains why dissection entry tears often begin transversely [8, 28]. However, regional tensile strength of sinuses versus STJ versus AscAo were not reported.

Biomechanical aTAA wall properties have also been described based upon wall layer in addition to aortic region [28, 29], although such layer variations would be impossible at present to capture with *in vivo* clinical imaging. Deveja *et al.* [30] studied biomechanical properties of aneurysmal wall as a whole and separate intimal, medial and adventitial layers. Failure longitudinal wall stresses in TAV-aTAAs were ∼800 kPa at the intima, ∼200 kPa at the media and ∼1300 kPa at the adventitia. Intact wall longitudinal failure stress was ∼700 kPa. Sokolis *et al.* [28] found regional variation of human aTAA mechanical properties from surgical tissue samples. Anterior aTAA wall was weaker than either the right or left lateral walls but not the posterior wall. No other regional differences were noted. No studies have compared wall strength of AscAo versus sinuses versus STJ. Our preliminary data suggests STJ is weaker than sinuses in normal aorta. As such, higher stresses in the sinuses may be compensated by greater strength. When examining peak walls stresses in STJ versus AscAo exclusively, longitudinal peak stresses occurred in greater frequency in the STJ 202 (87%) than AscAo 30 (13%). Larger population studies of wall strength and regional variation are required. For clinical application of FE models, understanding patient-specific aTAA wall stresses will be valuable for determining dissection risk when coupled with comprehensive population wall strength data.

Limitations

This veteran population study was predominantly male (97%) and thus does not apply to women. Furthermore, the veteran risk profile carries a larger percentage of risk factors for aTAAs including hypertension, hyperlipidaemia and smoking and thus may not be representative of the general civilian aTAA population. In addition, we focused on wall stresses due to hydrostatic forces from blood pressure rather than wall shear stresses as they are 5 orders of magnitude larger [15]. As such the impact of wall shear stresses on our wall stresses would be minimal. Wall shear stresses and helical flows are primarily deranged in BAV-associated aTAA. BAV disease has been found to have elevated wall shear stresses in aTAA which correlated with medial degeneration. This could possibly lead to aneurysm growth or changes in wall strength, but that population was excluded in this study. Fluid–structure interaction (FSI) simulations were beyond the scope of the study. Lastly, averaged TAV-aTAA material properties from prior stretch testing were used uniformly across aortic regions. We previously found that wall stresses were not significantly different when averaged versus patient-specific material properties were used [16].

CONCLUSION

We described patient-specific TAV-aTAA wall stress profiles and found that sinuses and STJ experienced significantly larger circumferential and longitudinal wall stresses than AscAo. Similarly, stresses along the lesser curvature were larger than along the greater curvature. Our results suggest regions of greater wall stresses where if the peak magnitudes substantially exceeded normal values or exceeded the wall strength in those regions, initial dissection tear could occur in TAV-aTAA patients. With better understanding of relative regional wall strength, FE modelling could be studied prospectively to determine the wall stress cut-offs for dissection similar to diameter cut-offs. Patient-specific wall stress assessments could then be applied to determine patient-specific dissection risk based on wall stress to wall strength ratios and aid in the decision-making of elective surgical TAV-aTAA repair.

Funding

This work was supported by the National Institutes of Health [R01HL119857-01A1 to E.E.T. and L.G.]; the American Heart Association Postdoctoral fellowship [20POST35211107 to Z.W.]; and National Institutes of Health [K25HL150408 to Y.X.].

Conflict of interest: none declared.

Author contributions

Axel Gomez: Data curation; Formal analysis; Validation; Writing—original draft. **Zhongjie Wang:** Data curation; Formal analysis; Investigation; Methodology; Validation; Writing—review & editing. **Yue Xuan:** Data curation; Formal analysis; Methodology; Supervision; Validation; Writing—review & editing. **Michael D. Hope:** Data curation; Investigation; Methodology; Resources; Visualization; Writing—review & editing. **David A. Saloner:** Data curation; Funding acquisition; Methodology; Visualization; Writing—review & editing. **Julius M. Guccione:** Conceptualization; Formal analysis; Funding

acquisition; Methodology; Project administration; Supervision; Writing—review & editing. **Liang Ge:** Conceptualization; Data curation; Funding acquisition; Investigation; Methodology; Project administration; Resources; Software; Supervision; Validation; Writing—review & editing. **Elaine E. Tseng:** Conceptualization; Investigation; Methodology; Project administration; Resources; Software; Supervision; Writing—review & editing.

Reviewer information

Interactive CardioVascular and Thoracic Surgery thanks Sven Peterss, Santi Trimarchi and the other, anonymous reviewer(s) for their contribution to the peer review process of this article.

REFERENCES

[1] Gomez A, Wang Z, Xuan Y, Wisneski AD, Hope MD, Saloner DA *et al.* Wall stress distribution in bicuspid aortic valve-associated ascending thoracic aortic aneurysms. Ann Thorac Surg 2020;110:807–14.

[2] Guo MH, Appoo JJ, Saczkowski R, Smith HN, Ouzounian M, Gregory AJ *et al.* Association of mortality and acute aortic events with ascending aortic aneurysm: a systematic review and meta-analysis. JAMA Netw Open 2018;1:e181281.

[3] Conzelmann LO, Weigang E, Mehlhorn U, Abugameh A, Hoffmann I, Blettner M *et al.* Mortality in patients with acute aortic dissection type A: analysis of pre- and intraoperative risk factors from the German Registry for Acute Aortic Dissection Type A (GERAADA). Eur J Cardiothorac Surg 2016;49:e44–52.

[4] Pape LA, Awais M, Woznicki EM, Suzuki T, Trimarchi S, Evangelista A *et al.* Presentation, diagnosis, and outcomes of acute aortic dissection: 17-year trends from the International Registry of Acute Aortic Dissection. J Am Coll Cardiol 2015;66:350–8.

[5] Hiratzka LF, Bakris GL, Beckman JA, Bersin RM, Carr VF, Casey DE Jr *et al.* 2010 ACCF/AHA/AATS/ACR/ASA/SCA/SCAI/SIR/STS/SVM Guidelines for the diagnosis and management of patients with thoracic aortic disease. A report of the American College of Cardiology Foundation/American Heart Association Task Force on Practice Guidelines, American Association for Thoracic Surgery, American College of Radiology, American Stroke Association, Society of Cardiovascular Anesthesiologists, Society for Cardiovascular Angiography and Interventions, Society of Interventional Radiology, Society of Thoracic Surgeons, and Society for Vascular Medicine. J Am Coll Cardiol 2010;55:e27–129.

[6] Pape LA, Tsai TT, Isselbacher EM, Oh JK, O'Gara PT, Evangelista A *et al.* Aortic diameter >or = 5.5 cm is not a good predictor of type A aortic dissection: observations from the International Registry of Acute Aortic Dissection (IRAD). Circulation 2007;116:1120–7.

[7] Rylski B, Branchetti E, Bavaria JE, Vallabhajosyula P, Szeto WY, Milewski RK *et al.* Modeling of predissection aortic size in acute type A dissection: more than 90% fail to meet the guidelines for elective ascending replacement. J Thorac Cardiovasc Surg 2014;148:944–8.e1.

[8] Jaussaud N, Chitsaz S, Meadows A, Wintermark M, Cambronero N, Azadani AN *et al.* Acute type A aortic dissection intimal tears by 64-slice computed tomography: a role for endovascular stent-grafting? J Cardiovasc Surg (Torino) 2013;54:373–81.

[9] Pichamuthu JE, Phillippi JA, Cleary DA, Chew DW, Hempel J, Vorp DA *et al.* Differential tensile strength and collagen composition in ascending aortic aneurysms by aortic valve phenotype. Ann Thorac Surg 2013;96:2147–54.

[10] Gee MW, Förster C, Wall WA. A computational strategy for prestressing patient-specific biomechanical problems under finite deformation. Int J Numer Methods Biomed Eng 2010;26:52–72.

[11] Wang Z, Flores N, Lum M, Wisneski AD, Xuan Y, Inman J *et al.* Wall stress analyses in patients with ≥5 cm versus <5 cm ascending thoracic aortic aneurysm. J Thorac Cardiovasc Surg 2020. In Press.

[12] Wang Z, Xuan Y, Guccione JM, Tseng EE, Ge L. Impact of patient-specific material properties on aneurysm wall stress: finite element study. J Heart Valv Dis 2018-19;27:275–284.

[13] Speelman L, Bosboom EM, Schurink GW, Hellenthal FA, Buth J, Breeuwer M *et al.* Patient-specific AAA wall stress analysis: 99-percentile versus peak stress. Eur J Vasc Endovasc Surg 2008;36:668–76.

[14] Nathan DP, Xu C, Plappert T, Desjardins B, Gorman JH 3rd, Bavaria JE *et al.* Increased ascending aortic wall stress in patients with bicuspid aortic valves. Ann Thorac Surg 2011;92:1384–9.

[15] Pasta S, Rinaudo A, Luca A, Pilato M, Scardulla C, Gleason TG *et al.* Difference in hemodynamic and wall stress of ascending thoracic aortic aneurysms with bicuspid and tricuspid aortic valve. J Biomech 2013;46:1729–38.

[16] Nathan DP, Xu C, Gorman JH, Fairman RM, Bavaria JE, Gorman RC *et al.* Pathogenesis of acute aortic dissection: a finite element stress analysis. Ann Thorac Surg 2011;91:458–63.

[17] Trabelsi O, Davis FM, Rodriguez-Matas JF, Duprey A, Avril S. Patient specific stress and rupture analysis of ascending thoracic aneurysms. J Biomech 2015;48:1836–43.

[18] Xuan Y, Wang Z, Liu R, Haraldsson H, Hope MD, Saloner DA *et al.* Wall stress on ascending thoracic aortic aneurysms with bicuspid compared with tricuspid aortic valve. J Thorac Cardiovasc Surg 2018;156:492–500.

[19] Emerel L, Thunes J, Kickliter T, Billaud M, Phillippi JA, Vorp DA *et al.* Predissection-derived geometric and distensibility indices reveal increased peak longitudinal stress and stiffness in patients sustaining acute type A aortic dissection: implications for predicting dissection. J Thorac Cardiovasc Surg 2019;158:355–63.

[20] Capoulade R, Teoh JG, Bartko PE, Teo E, Scholtz JE, Tastet L *et al.* Relationship between proximal aorta morphology and progression rate of aortic stenosis. J Am Soc Echocardiogr 2018;31:561–9.e1.

[21] Beller CJ, Labrosse MR, Thubrikar MJ, Szabo G, Robicsek F, Hagl S. Increased aortic wall stress in aortic insufficiency: clinical data and computer model. Eur J Cardiothorac Surg 2005;27:270–5.

[22] Etz CD, von Aspern K, Hoyer A, Girrbach FF, Leontyev S, Bakhtiary F *et al.* Acute type A aortic dissection: characteristics and outcomes comparing patients with bicuspid versus tricuspid aortic valve. Eur J Cardiothorac Surg 2015;48:142–50.

[23] Januzzi JL, Isselbacher EM, Fattori R, Cooper JV, Smith DE, Fang J *et al.* Characterizing the young patient with aortic dissection: results from the International Registry of Aortic Dissection (IRAD). J Am Coll Cardiol 2004;43:665–9.

[24] Nissen AP, Ocasio L, Tjaden BL Jr, Sandhu HK, Riascos RF, Safi HJ *et al.* Imaging characteristics of acute type A aortic dissection and candidacy for repair with ascending aortic endografts. J Vasc Surg 2019;70:1766–75.e1.

[25] Plonek T, Zak M, Rylski B, Berezowski M, Czerny M, Beyersdorf F *et al.* Wall stress correlates with intimal entry tear localization in type A aortic dissection. Interact CardioVasc Thorac Surg 2018;27:797–801.

[26] Waldo KL, Hutson MR, Ward CC, Zdanowicz M, Stadt HA, Kumiski D *et al.* Secondary heart field contributes myocardium and smooth muscle to the arterial pole of the developing heart. Dev Biol 2005;281:78–90.

[27] Forsell C, Bjorck HM, Eriksson P, Franco-Cereceda A, Gasser TC. Biomechanical properties of the thoracic aneurysmal wall: differences between bicuspid aortic valve and tricuspid aortic valve patients. Ann Thorac Surg 2014;98:65–71.

[28] Iliopoulos DC, Deveja RP, Kritharis EP, Perrea D, Sionis GD, Toutouzas K *et al.* Regional and directional variations in the mechanical properties of ascending thoracic aortic aneurysms. Med Eng Phys 2009;31:1–9.

[29] Azadani AN, Chitsaz S, Matthews PB, Jaussaud N, Leung J, Tsinman T *et al.* Comparison of mechanical properties of human ascending aorta and aortic sinuses. Ann Thorac Surg 2012;93:87–94.

[30] Deveja RP, Iliopoulos DC, Kritharis EP, Angouras DC, Sfyris D, Papadodima SA *et al.* Effect of aneurysm and bicuspid aortic valve on layer-specific ascending aorta mechanics. Ann Thorac Surg 2018;106:1692–701.